

CURRENT DISTRIBUTION OF GROUNDING GRID CONDUCTORS BURIED IN TWO-LAYER SOIL SYSTEM

Osama E. GOUDA

Faculty of Engineering, Cairo University,
Cairo, Egypt.
Prof_ossama11@yahoo.com

Sobhy S. DESSOUKY

Faculty of Engineering, Port Said University,
Port Said, Egypt.
sobhyserry@yahoo.com

Ahmed El. KALAS

Faculty of Engineering, Port Said University,
Port Said, Egypt.
Kalas_14@yahoo.com

Mohamed A. HAMDY

Faculty of Technology, Worker's University,
Ismailia, Egypt.
enghamdym@yahoo.com

Abstract: For safety and stable operation of electrical system purposes, grounding grid has been used. The current distribution of such grounding grid conductors is more likely calculated by analytical or numerical methods. This paper presents a new contribution to obtain the current distribution of grounding grid conductors with and without vertical rods buried in two-layer soil. The two-layer soil model has been simulated mathematically using two suitable values of resistivity. The indicated results of this paper give the current distribution for each segment of each mesh with and without driving rods. The effect of vertical rods, which has connected to horizontal grounding grid on current distribution and grounding resistance, has been studied. For increasing the flexibility of current distribution calculations of grounding grids, per unit system has been used in this paper. An experimental model to simulate two-layer soil is presented for the validation of the calculated results.

Keywords: Current Distribution, Grounding Grid, Two-Layer Soil, Mathematical Model.

1. Introduction

Grounding is necessary for the safe and reliable operation of power systems. Grounding systems analysis, including buried grids and driven rods, have been the subject of many recent papers [1 -9]. The grounding resistance is one of the most important parameters of ground electrodes; thus, the current

distribution among various parts of substation grounding systems has been affected by different parameters of grounding systems. Hence, the grounding resistance should be estimated in early design and the performance of the grounding grid is very important to the substation [10].

Many studies have analyzed the performance of the grounding grid, most mainly presenting their results with the slight introduction of their methods. Only a few works can provide details of the current distribution analysis of the grounding grid conductors [11–14].

R. J. Heppe [15], suggested a method to get the grids current distribution, but he assumed that the current densities of all segments of grounding grid are equal to simplify the computations of surface voltage of grounding grid. In IEEE 80 [9], for example, a mathematical analysis has been presented for the surface voltage gradient calculation using the assumptions that the currents are the same in each conductor; both are near the edge or near the center of the grounding grid. IEEE 80 assumed that the currents are the same at all points on each conductor, and the cross-conductors have a negligible effect. Nevertheless, in the real case, the current density from the grid conductors to the surrounding soil varies because of the proximity of nearby parallel and/or cross conductors and because of end effects. In a uniformly spaced grid, the current density is smallest near the center of the grid and highest at the edges and corners. Yan Gan and Jiangjun Ruan [16] used the

electromagnetic field theory (FEM) to calculate the current distribution of grounding grid conductors. Similar studies are done using electromagnetic field theory in references [17-19]

In this paper, the mathematical method has been presented to calculate current distribution in all segments of grounding grid with different dimensions and a different number of meshes of grounding grid with and without vertical rods buried in two layers soil resistivity.

2. Mathematical model

In order to find the current distribution of two layers soil resistivity. First of all the apparent soil resistivity ρ_a is calculated [9, 16], and [17], then the grounding grid is divided into many segments, the current density will be assumed constant within each segment of the grounding grid segments, but will be allowed to be different from segment to segment.

Fig.1. gives the flowchart used in the calculation of current distribution in the proposed technique. According to the previous references [20, 21], in two layers soil, Eq. 1. can be used to calculate the apparent soil resistivity ρ_a for the grounding grids without rods. However, the grounding grids, which have been buried in the top layer and the rods have been driven to reach to the second layer, the apparent soil resistivity ρ_a can be calculated in this case by using Eq. 2., [9].

$$\rho_a = \frac{\rho_1}{\left[1 + \left[\left(\frac{\rho_1}{\rho_2} \right) - 1 \right] \left[1 - e^{-\frac{1}{K(D+2H)}} \right] \right]} \quad (1)$$

$$\rho_a = [L_r(\rho_1 \rho_2)] / [\rho_2 (D-H) + \rho_1 (L_r + H-D)] \quad (2)$$

Where, ρ_a , ρ_1 , and ρ_2 are the apparent resistivity, resistivity of upper and lower soil respectively, D is the top layer thickness, H is the grid laying depth,

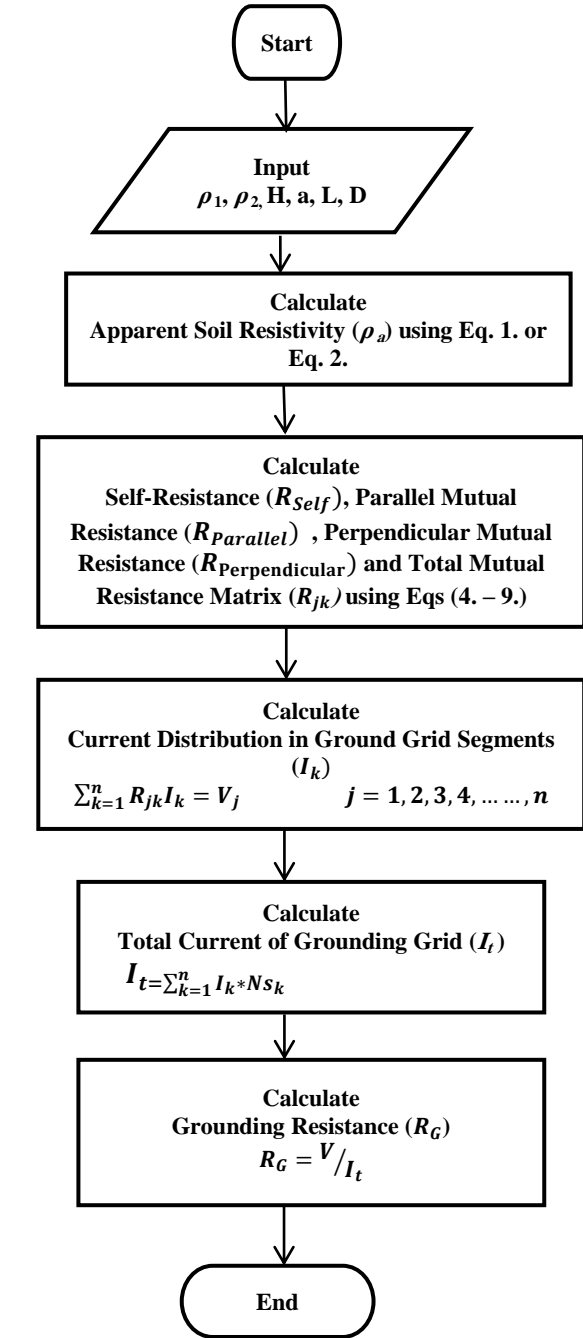


Fig.1. Current distribution in proposed technique flowchart

L_r is the length of each rod and K is the reflection factor which is defined by using Eq. 3.

$$K = (\rho_2 - \rho_1) / (\rho_2 + \rho_1) \quad (3)$$

The self-resistance of a segment R_{Self} is the ratio of the voltage on a segment to the current that will flow out of it, neglecting the effects of other segments.

For the computation of the self-resistance of conductor segment of length L , Eq. 4. is used [15]:

$$R_{Self} = \left[\frac{\rho_a}{2\pi L^2} \right] \times \left[L \ln \left(\frac{\sqrt{L^2+a^2}+L}{a} \times \frac{\sqrt{L^2+a^2+4H^2}+L}{\sqrt{a^2+4H^2}} \right) + a + \sqrt{a^2+4H^2} - \sqrt{L^2+a^2} - \sqrt{L^2+a^2+4H^2} \right] \quad (4)$$

Where:

- L is the length of the conductor segment in (m)
- a is the radius of the conductor segment in (m)
- H is the grid laying depth in (m)
- ρ_a is the apparent soil resistivity in (Ω -m)
- R_{Self} is the self- resistance of conductor segment in (Ω)

If two segments of the grounding grid AB and EF are parallel segments with length of L_1, L_2 respectively and letting the x-axis lie along segment AB with the origin at point A, and letting x, y, z be the coordinates of point E, as given in Fig. 2 -a. of parallel conductor segments. Parallel mutual resistance $R_{Parallel}$ is computed by using Eq. 5., [15]:

$$R_{Parallel} = \frac{M_{Parallel} \times \rho_a}{4\pi \times L_1 \times L_2} \quad (5)$$

Where $M_{Parallel}$ is a coefficient which can be indicated using Eq. 6.:

$$M_{Parallel} = L_1 \ln \frac{\sqrt{(x+L_2-L_1)^2+w^2}+x+L_2-L_1}{\sqrt{(x-L_1)^2+w^2}+x-L_1} + (x+L_2) \ln \frac{\sqrt{(x+L_2-L_1)^2+w^2}-(x+L_2-L_1)}{\sqrt{(x+L_2)^2+w^2}-(x+L_2)} - x \ln \frac{\sqrt{(x-L_1)^2+w^2}-(x-L_1)}{\sqrt{x^2+w^2}-x} - \sqrt{(x-L_1)^2+w^2} - \sqrt{(x+L_2)^2+w^2} + \sqrt{(x+L_2-L_1)^2+w^2} + \sqrt{(x)^2+w^2} \quad (6)$$

Where: $W^2 = y^2 + z^2$

There are two values of $R_{Parallel}$ have to be computed and added to investigate the effect of the surface image, the first is the resistance of the two conductor segments themselves, and the second is the mutual resistance between one conductor segment and the image of the other. This can conveniently be done by calling the mutual resistance subroutine twice, once with $z = 0$, and the other with $z = 2 \times H$.

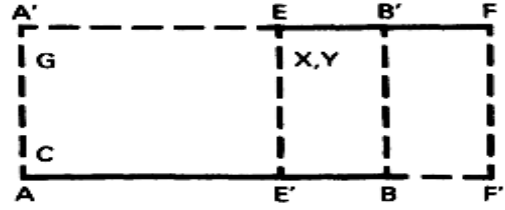


Fig. 2 -a. Parallel conductor segments

If AB and EF segments are perpendicular with lengths of L_1, L_2 respectively, and again letting the x-axis lie along segment AB with the origin at point A, and letting x, y, z be the coordinates of point E, as given in Fig. 2 -b of Perpendicular conductor segments.

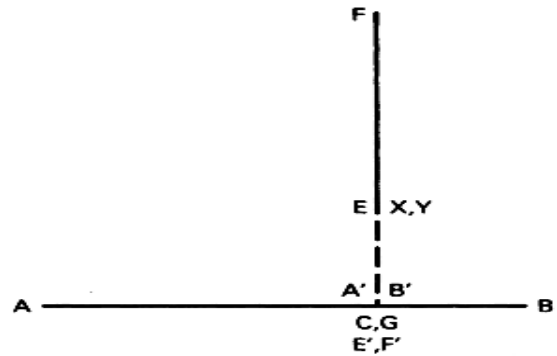


Fig. 2 -b. Perpendicular conductor segments

Perpendicular mutual resistance $R_{Perpendicular}$ can be computed by using Eq. 7., [15]:

$$R_{Perpendicular} = \frac{M_{Perpendicular} \times \rho_a}{4\pi \times L_1 \times L_2} \quad (7)$$

Where $M_{Perpendicular}$ is a coefficient, which can be indicated using Eq. 8.:

$$M_{Perpendicular} = (L_1 - x) \ln \left(\frac{\sqrt{(L_1-x)^2+(L_2+y)^2+z^2}+L_2+y}{\sqrt{(L_1-x)^2+y^2+z^2}+y} \right) + (x) \ln \left(\frac{\sqrt{x^2+(L_2+y)^2+z^2}+L_2+y}{\sqrt{x^2+y^2+z^2}+y} \right) + (L_2 + y) \ln \left(\frac{\sqrt{(L_1-x)^2+(L_2+y)^2+z^2}+L_1-x}{\sqrt{x^2+(L_2+y)^2+z^2}-x} \right) - (y) \ln \left(\frac{\sqrt{(L_1-x)^2+y^2+z^2}+L_1-x}{\sqrt{x^2+y^2+z^2}-x} \right) - |U| \quad (8)$$

Where: $U = 0$ if $z = 0$, and if $z \neq 0$, U can be computed using Eq. 9.:

$$U = (z) \left[\tan^{-1} \left(\frac{(L_1-x)(L_2+y)}{(z) \sqrt{(L_1-x)^2 + (L_2+y)^2 + z^2}} \right) - \right. \\ \left. \tan^{-1} \left(\frac{(L_1-x)(y)}{(z) \sqrt{(L_1-x)^2 + y^2 + z^2}} \right) - \right. \\ \left. \tan^{-1} \left(\frac{(-x)(L_2+y)}{(z) \sqrt{x^2 + (L_2+y)^2 + z^2}} \right) + \tan^{-1} \left(\frac{(-x)(y)}{(z) \sqrt{x^2 + y^2 + z^2}} \right) \right] \quad (9)$$

After the calculations of self, parallel and perpendicular resistances, total mutual resistance matrix R_{jk} has been performed and the values of the current of each segment of grounding grid I_k can be obtained by solving the following set of simultaneous linear equations:

$$\sum_{k=1}^n R_{jk} I_k = V_j \quad j = 1, 2, 3, 4, \dots, n \quad (10)$$

Where:

- R_{jk} is the total resistance matrix of self and mutual resistance values in (Ω)
- I_k is the list of currents induced in the n types of segments in (A)
- V_j is the list of voltages applied to the n segments in (Volt)

It will be assumed herein that all of the segments are at the same voltage; this is usually permissible at power frequencies because the resistance and inductive reactance of the wires are small compared to the resistance between the segments and the earth. If one is interested in the response of the grid to brief transients, such as those associated with lightning surges, inductive effects become important [15]. Equation 10. states that the sum of the voltages induced into a segment by its own leakage current and the leakage currents from all other segments must be equal to the applied voltage (V_j).

The total current of the grounding grid (I_t) in a grid with n segment current types can be obtained using Eq. 11.:

$$I_t = \sum_{k=1}^n I_k N S_k \quad (11)$$

Where:

- I_t is the total current in the grounding grid in (A)
- I_k is the current in each segment in (A)
- n is the number of segment current types
- $N S_k$ is the number of segments of the same current type

After the investigation of the total current of grounding grid, the grounding resistance of the grid (R_G) can be obtained using Eq. 12.:

$$R_G = V / I_t \quad (12)$$

Where:

- R_G is the grounding resistance in (Ω)
- V is the list of voltages applied to the n segments in (Volt)
- I_t is the total current in the grounding grid in (A)

3. Numerical generalization study

For the purposes of increasing the flexibility of the calculations of this study, the per-unit system has been used as a general computation by taking:

$$KVA_{Base} = 100 \text{ KVA, and } KV_{Base} = 10 \text{ KV.} \\ I_{Base} = KVA_{Base} / KV_{Base}, \\ R_{Base} = (KV_{Base})^2 \times 1000 / KVA_{Base}. \text{ Then,} \\ R_{p.u.} = R / R_{Base} \text{ and} \\ V_{p.u.} = V / KV_{Base} \times 1000.$$

The system parameters will be considered as upper layer soil resistivity $\rho_1 = 33 \Omega \cdot \text{m}$ and lower layer soil resistivity $\rho_2 = 19 \Omega \cdot \text{m}$, with reflection factor $K = -0.2692$. Apparent soil resistivity has been calculated using Eq. 2: $\rho_a = 25 \Omega \cdot \text{m}$. Length of each segment $L = 8 \text{ m}$ (conductors and rods). The depth of burial of grounding grid $H = 0.5 \text{ m}$. The top layer thickness $D = 5 \text{ m}$. Conductor radius $a = 0.007 \text{ m}$ (4/0 wire). List of voltages applied to the n segments $V = 1.5 \text{ p.u.}$ (assumed constant).

3.1. Grounding grids without rods

By dividing (1×1) grounding grid with one mesh into four segments with same segment type and same current as shown in Fig. 3-a.:

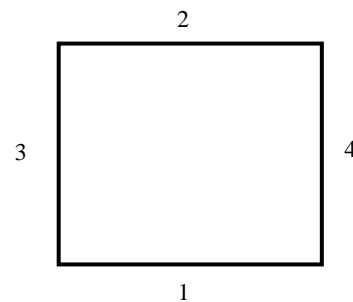


Fig. 3-a. Grounding grid (1×1) (four conductors)

Different mutual resistances (self, parallel and perpendicular) can be found by using Eqs. 4., 5. and 7., respectively:

$$R_1 = R_{Self} = 0.0057 \text{ p.u.} \\ R_2 = R_{Parallel} = 6.1129 \times 10^{-4} \text{ p.u.}$$

$$R_3 = R_4 = R_{\text{perpendicular}} = 0.0011 \text{ p.u.}$$

Total grounding grid mutual resistances are:

$$R_{jk} = R_1 + R_2 + R_3 + R_4 = 0.0085 \text{ p.u.}$$

The current of each segment can be calculated using Eq. 10. as shown in Fig. 3-b.:

$$I = 177.1477 \text{ p.u.}$$

Then the total grounding grid current has been calculated using Eq. 11.:

$$I_t = 708.5907 \text{ p.u.}$$

Grounding resistance is calculated by using Eq. 12.:

$$R_G = 0.0021 \text{ p.u.}$$

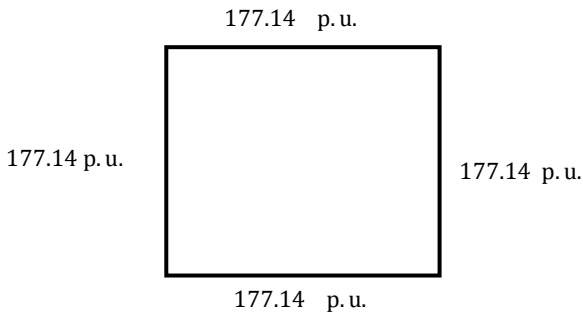


Fig. 3- b Grounding grid (1×1) current distribution

In (2 × 2) grounding grid with four meshes without vertical rods, the grid has been divided into 12 segments with two types of segment current types (type one from segment no. 1 to segment no. 8 and type two from segment no.9 to segment no.12). Different mutual resistances (self, parallel and perpendicular) must be found by using Eqs. 4., 5. and 7. Then the total mutual resistance matrix (R_{jk}) is:

$$R_{jk} = \begin{bmatrix} R_{11} & R_{12} \\ R_{21} & R_{22} \end{bmatrix}$$

$$R_{jk} = \begin{bmatrix} 0.0094 & 0.0026 \\ 0.0052 & 0.0069 \end{bmatrix} \text{ p.u.}$$

The current of each segment of the two segment current types in (p.u.) can be calculated by using Eq. 10. as shown in Fig. 4.:

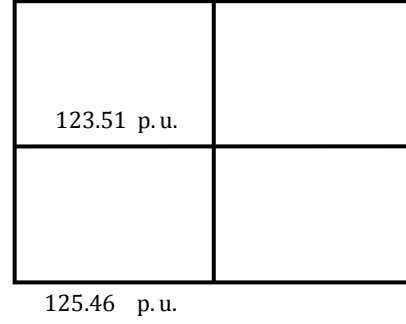


Fig. 4. Grounding grid (2×2) current distribution

The total grounding grid current is obtained by using Eq. 11:

$$I_t = 1497.7 \text{ p.u.}$$

Then the grounding resistance is calculated by using Eq. 12:

$$R_G = 0.0010 \text{ p.u.}$$

In (3×3) grounding grid with nine meshes without vertical rods, the grid has been divided into 24 segments with four types of segment current types. Type one from segment no.1 to segment no. 8, type two from segment no. 9 to segment no. 12, type three from segment no.13 to segment no. 20 and type four from segment no.21 to segment no.24. Different mutual resistances (self, parallel and perpendicular) must be found by using Eqs. 4., 5. and 7. respectively, the total mutual resistance matrix (R_{jk}) in (p.u.) is:

$$R_{jk} = \begin{bmatrix} 0.0083 & 0.0014 & 0.0037 & 0.0015 \\ 0.0036 & 0.0068 & 0.0036 & 0.0016 \\ 0.0028 & 0.0019 & 0.0088 & 0.0024 \\ 0.0030 & 0.0024 & 0.0030 & 0.0085 \end{bmatrix}$$

The current passes through each segment in (p.u.) has been calculated using Eq. 10 as shown in Fig. 5.:

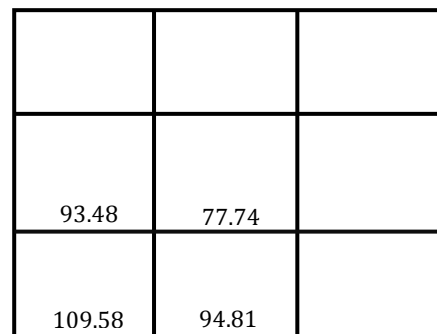


Fig. 5. Grounding grid (3×3) current distribution

Then the total grounding grid current can be obtained using Eq. 11.:

$$I_t = 2314.9 \text{ p.u.}$$

And the grounding resistance can be calculated using Eq. 12.:

$$R_G = 0.6480 \times 10^{-3} \text{ p.u.}$$

3.2. Grounding grids with rods

If the grounding grid has been connected to vertical rods, currents in all conductors and rods segments have been computed by the same method as shown below:

By dividing (1×1) grounding grid, with one mesh and four vertical rods into four conductors segments with the same segment current type (i_1) (from segment no.1 to segment no.4) and into four rods segments with another segment current type (i_2) (from segment no.5 to segment no.8) as shown in Fig. 6-a.:

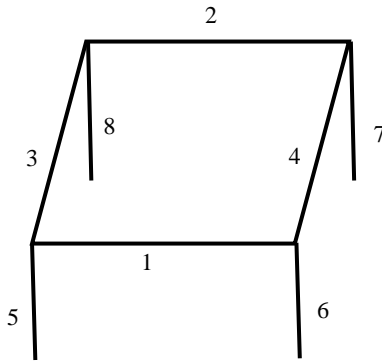


Fig. 6-a. Grounding grid (1×1) (4 conductors, 4 rods)

Different mutual resistances matrix R_{jk} can be found by using Eqs. 4., 5. and 7., the total mutual resistance matrix R_{jk} in (p.u.) is:

$$R_{jk} = \begin{bmatrix} R_{11} & R_{12} \\ R_{21} & R_{22} \end{bmatrix}$$

$$R_{jk} = \begin{bmatrix} 0.0085 & 0.0021 \\ 0.0026 & 0.0058 \end{bmatrix}$$

The current distribution of each grid segments in (p.u.) can be calculated using Eq. 10 as shown in Fig. 6-b.:

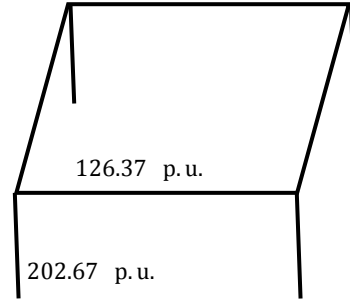


Fig. 6-b. Grounding grids (1×1) with 4 rods current distribution

The total grounding grid current has been calculated using Eq. 11.:

$$I_t = 1316.2 \text{ p.u.}$$

Then the grounding resistance is calculated using Eq. 12.:

$$R_G = 0.0011 \text{ p.u.}$$

In (2×2) grounding grid which has four meshes and nine vertical rods. The grid is divided into 21 segments with four types of segment current types (type one start at conductor segment no.1 to segment no.8, type two from conductor segment no.9 to segment no. 12, type three from rod segment no.13 to segment no.20 and rod segment no. 21 is type four). Each type segments have the same current passed through them.

Then different mutual resistances matrix (self, parallel and perpendicular) can be found by using Eqs. 4., 5. and 7., the total mutual resistance matrix R_{jk} in (p.u.) is:

$$R_{jk} = \begin{bmatrix} 0.0094 & 0.0026 & 0.0031 & 0.0003 \\ 0.0052 & 0.0069 & 0.0035 & 0.0001 \\ 0.0036 & 0.0016 & 0.0065 & 0.0004 \\ 0.0032 & 0.0026 & 0.0037 & 0.0043 \end{bmatrix}$$

The current distribution of each grid segments in (p.u.) have been calculated by using Eq. 10. as shown in Fig. 7.:

Then the total grounding grid current has been calculated by using Eq. 11.:

$$I_t = 2341.8 \text{ p.u.}$$

The grounding resistance can calculate using Eq. 12.:

$$R_G = 0.6405 \times 10^{-3} \text{ p.u.}$$

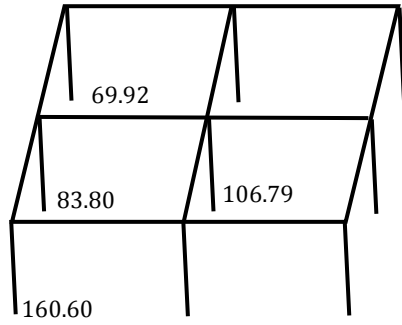


Fig. 7. Grounding grid (2×2) with nine rods current distribution in (p.u.)

In (3×3) grounding grid with nine meshes and 16 vertical rods. The grid is divided into 40 segments, with six types of segment current types. Type one start from the conductor segment no.1 to segment no.8, type two from conductor segment no.9 to segment no.12, type three from conductor segment no.13 to segment no.20, type four from conductor segment no.21 to segment no.24, type five from rod segment no.25 to segment no.36, and type six from rod segment no.37 to segment no.40. Each type segments have the same current passed through them, the total mutual resistance matrix R_{jk} in (p.u.) is:

$$R_{jk} = \begin{bmatrix} 0.0083 & 0.0017 & 0.0037 & 0.0017 & 0.0038 & 0.0013 \\ 0.0044 & 0.0068 & 0.0040 & 0.0016 & 0.0046 & 0.0007 \\ 0.0028 & 0.0021 & 0.0088 & 0.0029 & 0.0037 & 0.0019 \\ 0.0034 & 0.0024 & 0.0039 & 0.0085 & 0.0038 & 0.0021 \\ 0.0028 & 0.0015 & 0.0026 & 0.0012 & 0.0069 & 0.0010 \\ 0.0025 & 0.0013 & 0.0032 & 0.0026 & 0.0038 & 0.0058 \end{bmatrix}$$

The current distribution of each grid segments in (p.u.) has been calculated by using Eq. 10. as shown in Fig. 8.

The total grounding grid current is calculated using Eq. 11.:

$$I_t = 3205 \text{ p.u.}$$

Then the grounding resistance can be calculated using Eq. 12.:

$$R_G = 0.4680 \times 10^{-3} \text{ p.u.}$$

Similar results can be obtained for grids contain any number of meshes using the same steps given in the flowchart that drawn in Fig.1.

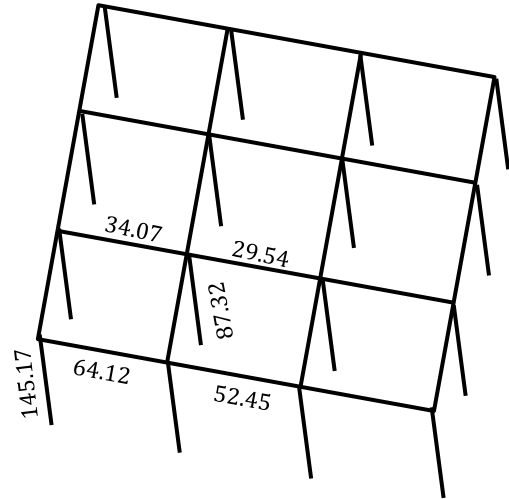


Fig.8. Grounding grid (3×3) with 16 rods current distribution

4. Comparison between grounding grids with and without vertical rods current distribution

Effects of using vertical rods connected to the horizontal grounding grid on current distribution have been displayed in Table 1., Table 2., and Table 3., Fig. 9, Fig.10, and Fig.11.

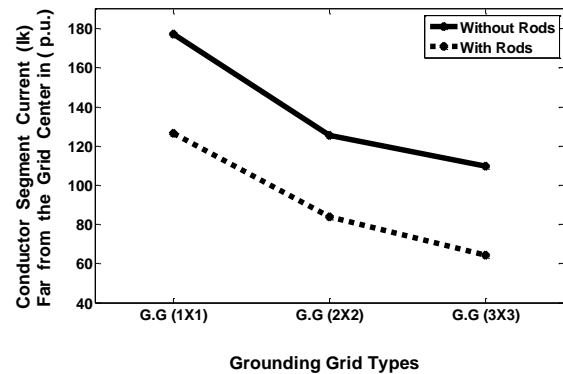


Fig. 9-a. Conductor segments current (I_k) in (p.u.) of grounding grids with different shapes with and without vertical rods

Table 1. Comparison between grounding grid (1×1) with and without vertical rod

Parameters	Grounding Grid Without Vertical Rods	Grounding Grid With Vertical Rods	
	Conductor	Conductor	Rod
Current of Each Segment (I_k) in (p.u.)	177.1477	126.3765	202.6722
Total Current of Grounding Grid (I_t) in (p.u.)	708.5907	1316.2	
Grounding Resistance to ground of Grounding Grid (R_G) in (p.u.)	0.0021	0.0011	

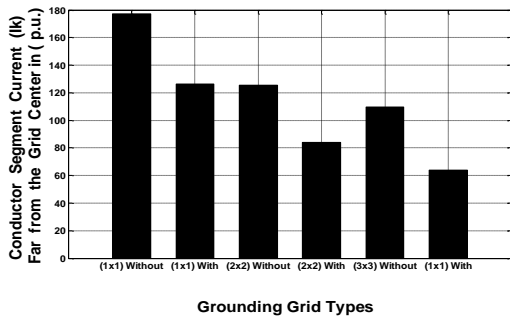


Fig.9-b. Conductor segments current (I_k) in (p.u.) comparison between grounding grids with different shapes with and without vertical rods

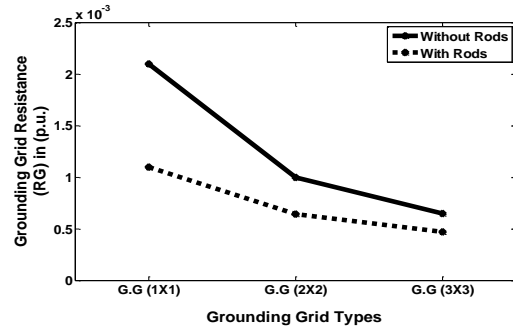


Fig. 11-a. Grounding grids resistance (R_G) in (p.u.) of grounding grids with different shapes with and without vertical rods

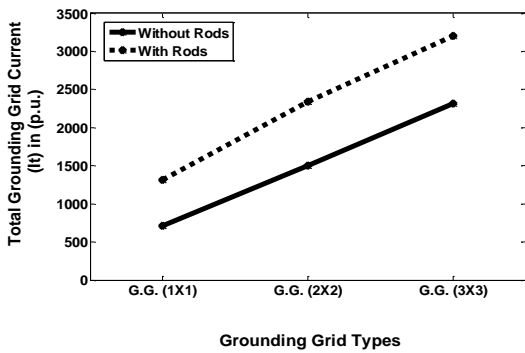


Fig. 10-a. Total grid current (I_t) in (p.u.) of grounding grids with different shapes with and without vertical rods

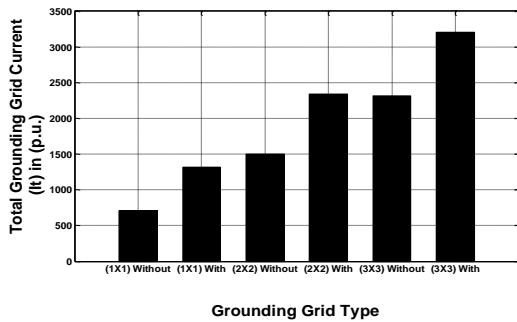


Fig. 10-b. Total grid current (I_t) in (p.u.) comparison between grounding grids with different shapes with and without vertical rods

Table 2. Comparison between grounding grid (2x2) with and without vertical rods

Parameters	Grounding Grid Without Vertical Rods		Grounding Grid With Vertical Rods			
	Conductor		Conductor		Rod	
	Near Center of G.G	Far Center for G.G	Near Center of G.G	Far Center for G.G	Near Center of G.G	Far Center for G.G
Current of Each Segment (I_k) in (p.u.)	123.51	125.46	69.92	83.80	106.79	160.60
Total Current of Grounding Grid (I_t) in (p.u.)	1497.7		2341.8			
Grounding Resistance to ground of Grounding Grid (R_G) in (p.u.)	0.0010		0.6405×10^{-3}			

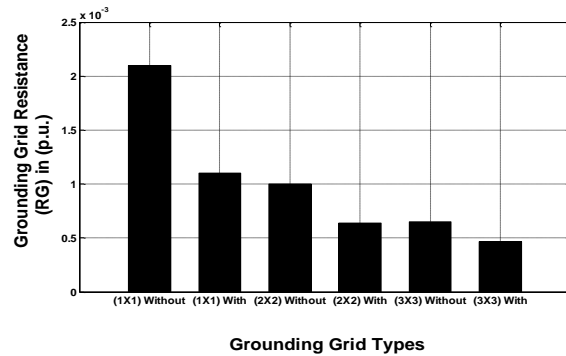


Fig. 11-b. Grounding grids resistance (R_G) in (p.u.) comparison between grounding grids with different shapes with and without vertical rods

Table 3. Comparison between grounding grid (3x3) with and without vertical rods

Parameters	Grounding Grid Without Vertical Rods		Grounding Grid With Vertical Rods			
	Conductor		Conductor		Rod	
	Near Center of G.G	Far Center for G.G	Near Center of G.G	Far Center for G.G	Near Center of G.G	Far Center for G.G
Current of Each Segment (I_K) in (p.u.)	93.48 77.74	109.58 94.81	34.07 29.54	64.12 52.45	87.32	145.17
Total Current of Grounding Grid (I_t) in (p.u.)	2314.9		3205			
Grounding Resistance to the ground of Grounding Grid (R_G) in (p.u.)	0.6480×10^{-3}		0.4680×10^{-3}			

From the obtained results, some of the percentage relations referring to grounding grid with and without vertical rods have been indicated:

- 1- The current distribution of the same conductor segments I_K is decreased in case of using vertical rods by the amount of 28.6% for (1x1). However, 43.38 % for near segments, 33.21 % for far segments of grid center of (2x2). In addition, 63.55 % for near segments, 41.48 % for far segments of grid center of (3x3) grounding grids.
- 2- The total currents of the grounding grids I_t with vertical rods are increased by the amount of 85.75 % for (1x1), 56.36 % for (2x2) and 38.45 % for (3x3) grounding grids.
- 3- The grounding grids with vertical rods resistance R_G are decreased by the amount of 47.62 % for (1x1), 35.95 % for (2x2) and 27.8 % for (3x3) grounding grids.

The calculated results are in agreement with that calculated by FEM [16].

5. Validation of the calculated results

5.1 Experimental setup

Figure 12. presents the experimental model to simulate two-layer soil. Glass electrolytic tank has dimensions of 1m x 1m x 0.5 m is used to simulate the two-layer soil. Tap water is used as an electrolyte, representing homogenous soil of each layer. The glass tank is divided into the top and bottom layers by conducting sheet. The inner surface

of top and bottom tank is covered by conducting sheath. The water resistivity can be changed by adding an adequate amount of salt. The electric resistivity of each layer is obtained by measuring the total dissolved salts.

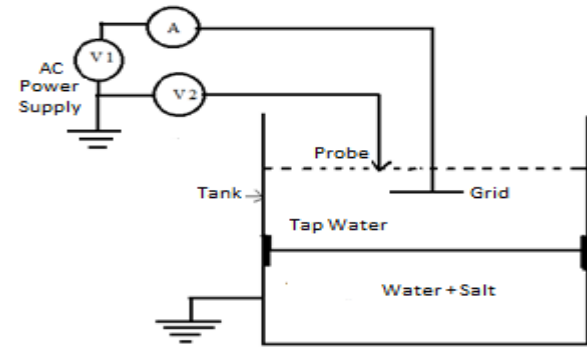


Fig. 12. Nonhomogeneous experimental setup

A voltmeter is used to measure the voltage that output from the autotransformer source and applied to the model of grounding grid (V_1). The magnitude of applied voltage is considered to be constant during the different tests; it is fixed in value equals to 150 volt in all cases. Another voltmeter is used to measure the surface potential (V_2), i.e along the diagonal of the grounding system in these tests. An ammeter is used to measure the current that following through the electrolyte between the model grid and the return electrode. A similar one with high accuracy and low resistance is used for measuring the current in each mesh conductor segment.

5.2 Experimental results

Tables 4. and 5. give the grounding grids current distribution with and without rods calculated and measured. The applied voltage to the grids in the model is 150 volt which is 1: 100 of the voltage used in the calculations (15 kV). The tested grids have dimensions of 8 cm x 8 cm, 16 cm x 16 cm and 24 cm x 24 cm. The scale factor is also 1:100 for selected grid dimensions. The length of vertical grounding electrode is 8 cm, and its radius is 0.7 mm. Also, the thickness of the first layer, in the nonhomogeneous experimental model is 5 cm. The water resistivity is adjusted by NaCl salt to be 0.33 Ohm. m for the top layer and 0.19 Ohm - m for the lower one to be 1: 100 scale factor compared with that used in the calculations.

From the results given in tables 4. and 5., it is noticed that the measured values are in agreement with that calculated, but in some measurements it is observed that the current value is less than the that calculated,

this may be is due to the resistance of the ammeter connected between segment parts for current measurement.

Table 4. Grounding grid current distribution without vertical rods as calculated and measured by using experimental model with scale factor 1: 100

parameters	One mesh (8 m ×8 m)	Four meshes (16 m ×16 m)	Nine meshes (24 m ×24m)
Current of each conductor segment located near to the grid center	---	123.5122 p.u. which is 1235.122 A calculated and 1197 A Experimental	93.4868 p.u., 934.868 A and 921 A Experimental 77.7481 p.u. 777.481 A and 754 A Experimental
Current of each conductor segment located far from the grid center	177.1477 p.u. which is 1771.477 A calculated and 1735 A Experimental	125.4614 p.u. which is 1254.614 A calculated and 1224 A Experimental	109.5887 p.u., 1095.887 A and 1080 A Experimental 94.8179 p.u., 948.179 A and 925 A Experimental
Total grounding grid current	7085.907 A and 7043 A Experimental	14977 A and 14935 A Experimental	23149 A and 23135 A Experimental

Table 5. Grounding grid current distribution with vertical rods as calculated and measured by using experimental model with scale factor 1: 100

parameters	One mesh (8 m ×8 m)	Four meshes (16 m ×16 m)	Nine meshes (24 m ×24m)
Current of each conductor segment located near to the grid center	---	69.9286 p.u. which is 699.286 A calculated and 660 A Experimental	34.0766 p.u., 340.766 A and 332 A Experimental 29.5457 p.u. , 295.457 A and 287 A Experimental
Current of each conductor segment located far from the grid center	126.3765 p.u. which is 1263.765 A calculated and 1251 A Experimental	83.8014 p.u. which is 838.014 A calculated and 812 A Experimental	64.1260 p.u., 641.260 A and 632 A Experimental 52.4500 p.u. , 524.500 A and 511 A Experimental
Current of each rod segment located near to the grid center	---	106.7969 p.u. which is 1067.969 A calculated and 1043 A Experimental	87.3273 p.u. which is 873.273 A calculated and 865 A Experimental
Current of each rod segment located far from the grid center	202.6722 p.u. which is 2026.722 A Calculated and 2014 A Experimental	160.6045 p.u. which is 1606.045 A calculated and 1592 A Experimental	145.1776 p.u. which is 1451.776 A calculated and 1447 A Experimental
Total grounding grid current	13162 A and 13130 A Experimental	23418 A and 23397 A Experimental	32050 And 32043 A Experimental

For more verification of the calculations done using the method of this paper, the calculated resistance of the grounding grids are compared with that obtained using Schwarz's equations [9] as given in Table VI.

Table 6. Comparison between grounding grid resistance (R_G) calculated using Schwarz's equations and proposed technique

The Grounding Resistance (R_G) in (p.u.)	G.G. (1×1) with 4 Rods	G.G. (2×2) with 9 Rods	G.G. (3×3) with 16 Rods
Schwarz's equations	0.0011	0.6597×10^{-3}	0.45017×10^{-3}
the proposed technique	0.0011	0.6405×10^{-3}	0.4680×10^{-3}
Differences %	0	2.9104×10^{-8}	3.9607×10^{-8}

According to Table 6., the percentage differences between Schwarz's equations and the proposed technique results in order to calculate the ground resistance (R_G) are so small, and below the acceptable difference limit 10%.

6. Conclusion

The analysis given in this paper permits the grounding mutual resistances of horizontal conductors and vertical rods forming grounding grid of complicated system to have been computed. The method uses modest amounts of programming time, computer time, and core memory even for rather large grids if they are symmetrical using the Mat-lab program. By analyzing the contribution performance results, it has been noted that using of vertical rods connected to horizontal grounding grid decrease the currents passed through each conductor and rod segments (I_K). However, the total current of grounding grid (I_t) increases and the grounding resistance of grounding grid (R_G) decreases in symmetric spaced grounding grid. The current of the segments near of the grounding grid center is lower than the currents far from the grounding grid center of any mesh numbers and this explains why it prefers to use non-equal spacing grids with concentrated conductors near the outer perimeter of the grids in grounding systems. The calculated and measured values are in agreement.

References

- [1] O. E. Gouda, A. Z. El Dein: *Ground Potential Rise of Faulty Substations having Equal and Unequal Spacing Grounding Grids Conductors*. In: IET Generation, Transmission & Distribution, 2017; Vol. 11, Issue 1, pp. 18 – 26.

- [2] W. Pan, H. Sun.: *Research Of Optimal Distance of External Grounding Grid*. In: IEEE International Conference 2016.
- [3] Zhu Yigang, Zhang Bo, Dong Yuxi.: *Measures for Optimized Voltage Balance Along Connection Line To External Grounding Device*. In: High Voltage Engineering, 2015; vol. 5, pp. 1-2.
- [4] B. Zhang, J. He, and Y. Jiang. "Safety Performance of Large Grounding Grid With Fault Current Injected From Multiple Grounding Points". IEEE Trans. 2015; Ind. Appl., vol. 51, no. 6, pp. 5116–5122.
- [5] A. Ackerman, P. K. Sen, and C. Oertli.: *Designing Safe And Reliable Grounding In AC Substations With Poor Soil Resistivity*. In: An Interpretation of IEEE Std. 80, IEEE Trans. 2013; Ind. Appl., vol. 49, no. 4, pp. 1883–1889.
- [6] J. A. Güemes, F. E. Hernandoc: *A Practical Approach for Determining the Ground Resistance of Grounding Grids*. In: IEEE Transaction on Power Delivery, 2006; Vol.21, No.3.
- [7] Z. Liping, Y. Jiansheng.: *Calculation of Substation Grounding Grids With Unequal Potential Model*. In: Proceedings of the CSEE, 2000; vol. 1, pp. 1-2.
- [8] *IEEE Guide for Measuring Earth Resistivity, Ground Impedance, and Earth Surface Potentials of a Ground System*. In: IEEE Std. 81-1983.
- [9] *IEEE Guide for Safety in AC Substation Grounding*. In: IEEE Std. 80 - 2000.
- [10] S. S. Dessouky, S.Ghoneim, S. Awad: *Grounding Resistance, Step and Touch Voltages for a Driven Vertical Rod into Two-Layer Model Soil*. In: International Conference on Power System Technology. 2010.
- [11] J.Yuan, H.Yang, L. Zhang, X. Cui, and X. Ma.: *Simulation Of Substation Grounding Grids With Unequal-Potential*. In: IEEE Trans., 2000; vol. 36, pp. 1468–1471.
- [12] F. P. Dawalibi: *Electromagnetic Fields Generated By Overhead and Buried Short Conductors Part 2—Ground Conductor*. In: IEEE Trans. Power Delivery, 1986; vol. PWRD-1, pp. 112–119.
- [13] L. Grcev, F. Dawalibi: *An Electromagnetic Model for Transients in Grounding Systems*. In: IEEE Trans. Power Delivery, 1990, vol. 5, pp.1773–1781.
- [14] A. F. Otero, J. Cidras, J. L. del Alamo: *Frequency-dependent Grounding System Calculation by Means of a Conventional Nodal Analysis Technique*. In: IEEE Trans. Power Delivery, 1999; vol. 14, pp. 873–878.
- [15] R. J. Heppe: *Computation of Potential at Surface above an Energized Grid or other Electrode, Allowing for Non-Uniform Current Distribution*. in: IEEE Transactions on Power Apparatus and Systems, 1979; Vol. PAS-98, No.6..
- [16] Y. Gan and J. Ruan: *Simulation of the Grounding Grid by Coupling the Uni-dimensional Finite Element Method (FEM) and the Three-dimensional FEM*. In: Progress in Electromagnetics Research Symposium 2005, Hangzhou, China, August 22-26, pp. 84- 88.
- [17] Zhant, L. P., J. S. Yuan, and Z. X. Li. : *The Complex Image Method and Its Application in the Simulation of Substation Grounding Grids*. In: Numerical Methods in Engin., Vol. 15, No. 11, 835-839, 1999.
- [18] Yuan, Jiansheng: *Simulation of Substation Grounding Grids with Unequal-potential*. In: IEEE Transactions on Magnetics, Vol. 36, No. 4, 2000.
- [19] Cardoso, Jose Roberto: *FEM Modeling of Grounded Systems with Ungrounded Approach*. In: IEEE Transactions on Magnetics, Vol. 30, No. 5, 1994.
- [20] J. A. Sullivan: *Alternative Earthling Calculations for Grids and Rods*. In: IEE Proceedings Transmission and Distributions, 1998; Vol. 145, No. 3, pp. 271 - 280,
- [21] J. Nahman, I. Paunovic; *Resistance To Earth Of Earthling Grids Buried In Multi-Layer Soil*. In: Electrical Engineering, Springer Verlag., 2005; pp. 281 - 287.